

Modelling Muddy Flash Floods and Debris Flows

B. NSOM, B. RAVELO, W. NDONG, N. LATRACHE

Université de Brest - IUT (LIME).LBMS EA 4325 - Rue de Kergoat..29231 BREST
FRANCE

K. BOUCLAGHEM, S. ELOURAGINI

Unité de Recherche « Energétique et Environnement » (03/ UR 13-06)
ISSAT de Sousse. Cité Taffala, 4003 SOUSSE Ibn Khaldoun
TUNISIA

Abstract – After long and intense rains in a mountainous region, large quantities of water flow in the torrents. For some reason, this flow can be obstructed by cross-linked branches and debris (natural dam). When the hydrostatic pressure exerted by the fluid exceeds a given yield value, the dam collapses and the fluid is released inside and outside the torrent bed, as well. Such scenario which is known as a dam-break flow can describe the initiation of certain geological flows, (debris flows, mudflows, etc.). As for any gravity current, the flow description depends on the time scale. Immediately after the dam collapse, the inertial forces are the dominant ones and this configuration can model a flash flood. Flash floods develop at time and space scales that conventional observation systems are not able to monitor, so reliable modelling remains a crucial step. At larger time scale, a viscous regime takes place where the viscous forces become the dominant ones and this configuration can model a classical debris flow. Debris floods develop in a long domain, i.e. a domain of space that is much longer than it is wide. They generally erode their bed and transport much energy and can move rocks and boulders upon very long distances. Both, the flash flows and the debris floods constitute dangerous phenomena for public safety and quality of life. The originality of the present approach is to consider these two flood waves as special cases of a single global model of a dam-break flow of a muddy fluid, depending on the time scale. The study was experimental, analytical and numerical, as well. The experimental study performed in previous work consisted in designing model fluids to be used in the laboratory experiments, characterizing these synthetic muds and monitoring the corresponding dam-break flows in the laboratory. The corresponding results agreed with the theoretical study presented here and which consists in stating the equations of motion governing the different flows studied, and solving them in their non dimensional form, both analytically and numerically.

Key-Words - Dam failure, Finite difference method, Herschel-Bulkley fluid, Inertial regime, Numerical models, One dimensional flow, Shallow water approximation, Similar solution, Viscous regime.

1 Background

Flood waves resulting from dam breaks have been responsible for the destruction of numerous structures and goods and for numerous losses of life. Such a flood wave may result from a dam failure caused by exceptional rainfall (e.g. Malpasset, France in 1959) or by an act of war (e.g. Dnieproghes, Ukraine in 1941). In order to appropriately size the dam and its associate structures, it is vital for the designers to accurately predict the development of the flow generated by the sudden water release after some gate malfunction or the failure of an upstream reservoir. Also, although the wave front travels fast, the spillway operators need to accurately estimate its arrival time in the downstream valley. Indeed, as shown in Table 1, the earlier the

warning is performed, the more efficiently the public safety is ensured.

In the nature, such scenario can describe the initiation of flash floods (e.g. Queensland event, Australia, 2001). After short but very intense rains over a small but sloping basin, a catastrophic quantity of water accumulates in the dales, invading the torrents and increasing the stage. If the draining network is insufficiently sized, a flash flood may result, with a travelling fast wave front causing severe damage in the downstream valley. While, in mountainous regions, after long and intense rains, debris flows can start in upper torrential catchments. They consist of water, clay and grains. They transport much energy and can even move rocks and boulders upon very long distances. These

violent phenomena can cause significant damage, especially when they spread on

the torrent alluvial fan.

| Dam name, place and year of event | Number of inhabitants exposed to the risk | Number of life losses | Elapsed time (hours) Between event and alert |
|--|---|-----------------------|--|
| Vega de Tera, Spain (1959) | 500 | 150 | 0 |
| Malpasset, France (1959) | 6000 | 421 | 0 |
| Buffalo Creek, Virginie W (1972) | 4000 | 125 | 1 |
| Black Hills, Dakota S (1972) | 17000 | 245 | 1 |
| Big Thompson, Colorado (1976) | 2500 | 139 | 1 |
| Laurel Run, Pensylvanie (1977) | 150 | 40 | 0 |
| Denver, Colorado (1965) | 3000 | 1 | 3 |
| Prospect Dam, Colorado 1980 | 100 | 0 | 5 |
| Bushy Hill Pond, Connecticut (1982) | 400 | 0 | 2-3 |
| Baldwin Hills, California (1983) | 16500 | 5 | 1.5 |
| DMAD, Utah (1983) | 500 | 1 | 1-12 |
| Northern New Jersey, New Jersey (1984) | 25000 | 2 | 2 |

Table 1: Dam-break events with life losses, [1].

In the laboratory, the study of a dam-break flow consists in considering a gate (located at $x=0$), obstructing a horizontal smooth channel, dry downstream and with a given quantity of fluid upstream (with height h_0), contained between a fix plate and a dam. At initial time, the dam collapses and the fluid is released downstream (positive wave), while a negative wave propagates upstream (negative wave). De Saint Venant [2] presented the equations governing the one-dimensional flow in a horizontal infinitely broad channel with vertical walls, assuming the shallow water

approximation. Ritter [3] gives the inviscid solution, stating that the wave front advances with a constant speed of $2\sqrt{gh_0}$, while the negative wave moves back with constant speed $\sqrt{gh_0}$. Between these two extremes, the average speed \tilde{u} and the hydrograph are respectively given by

$$\tilde{u} = \frac{2}{3} \left(\frac{x}{t} + \sqrt{gh_0} \right), \quad \sqrt{gh} = \frac{1}{3} \left(2\sqrt{gh_0} - \frac{x}{t} \right) \quad (1)$$

Important characteristics of the flow can be derived from these relations. At dam site,

height, average velocity and flow rate are constant and respectively given by

$$h_d = \frac{4}{9}h_0, \quad \tilde{u}_d = \frac{2}{3}\sqrt{gh_0} \quad (2)$$

$$q_d = h_d \tilde{u}_d = \frac{8}{27}\sqrt{gh_0^3} \quad (3)$$

To take viscous effects into account, Dressler [4] introduced a friction term dependent on the Chezy coefficient in these equations. This system was solved by Dressler [5], Whitham [6] and others. The Saint Venant equations are a hyperbolic system expressing the mass and the momentum conservation for a unit volume of water. They can also be solved numerically using the method of characteristics [7]. By recognizing relationships between total differentials of velocity and height with their partial derivatives, together with the Saint Venant equations, Faure and Nahas [8] used the finite difference method to numerically solve the dam-break problem for a viscous fluid, following Whitham's scheme in the front vicinity. Later, the equations governing the flow in the wave front vicinity. Later, the equations governing the flow in the front vicinity were treated either in their global form [9]) or in a undersimplified form [10]. While Hunt [11] built asymptotic solutions to the viscous dam-break problem.

Nsom carried out experiments with highly viscous Newtonian fluids, e.g., glucose syrup-water solutions using a horizontal [12] and a sloping channel [13]. He showed that both the inviscid (Ritter, [3]) and the similarity type of solution existed in each of the flow configurations considered. The inviscid type of solution was obtained immediately after the sudden collapse of the gate while the similarity type of solution governed the following times. He concluded that the dam-break problem consisted in two main classes of flow: the inertial flow, where the viscous terms in the momentum balance equation can be neglected (inviscid solution) and the viscous flow, where the inertial terms can be neglected (similar solution). In fact,

returning to the basic description of a dam-break flow, we can observe that it belongs to the large class of gravity currents. As such, its solution depends on time scale [14]. First of all, the inertial regime, characterized by a fixed height given by eq.7 at the dam-site (Ritter, [3]), holds immediately after the dam collapse. Then, this results in a solution dominated by viscous effects. The transition occurs when the negative wave touches the rear wall. A short time regime takes place until the wave reflected by the fixed plate overakes the front. This short time regime tends to an asymptotic form (long time solution). In the present model, the flash flood is governed by the inertial and the short time viscous solution, and the debris flow by the long time viscous solution.

Hunt [11] states that the Newtonian fluid can be used to model avalanches and debris flows. The inertial regime being governed by Ritter's solution, in the second section of this paper, both the short time and the long time solutions will be given for the Newtonian model of debris flows.

As noted previously, a muddy flash flood or debris flow is constituted of a complex mixture of water, clay and grains which is described as a continuum. In this aim, a general model for the open-channel flow of muddy fluids in a long space domain is presented in the third section. The conservation of mass and momentum equations are written in a non dimensional form with a shallow-water approximation. Herschel-Bulkley rheological behavior is assumed without neglecting any of the components of the stress tensor. In addition, no *a priori* value is assigned to the rheological parameters. A strongly non linear partial differential equation is obtained in a non dimensional form. The special cases of Newtonian and power law fluid are recovered by using appropriate corresponding values of the rheological parameters.

The solution for the muddy flash flood is provided in the fourth section while the

muddy debris flow is considered in the fifth section.

2 Newtonian model of debris flows

2.1 Problem statement

a. Equation of motion

Let h_0 denote the height of fluid at negative time in a smooth horizontal rectangular channel, g the gravity, ρ and μ the fluid density and viscosity, respectively. Using a cartesian system of coordinates with the origin at the dam site, x -axis lying on the channel-length and the z -axis in the increasing vertical direction (fig. 1).

The fluid is assumed to flow mainly in the direction of x -axis with height h at the given control section of the abscissa x , at time t . So, the vertical velocities are negligibly small, and therefore the pressure is hydrostatic, the pressure in the flow is given by

$$p = p_0 + \rho g(h - z) \tag{4}$$

where p_0 denotes the (constant) pressure at the free surface.

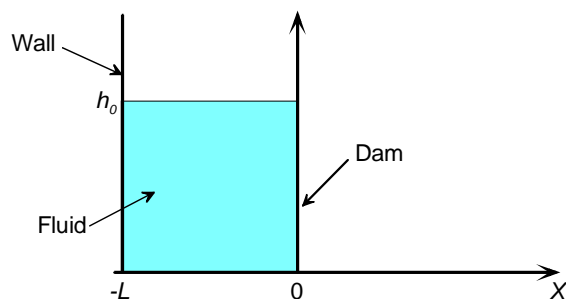


Fig 1: Configuration of horizontal dam-break flow at negative time

The balance between the pressure gradient and the viscous forces is thus expressed by

$$\frac{1}{\rho} \frac{\partial p}{\partial x} = g \frac{\partial h}{\partial x} = \nu \frac{\partial^2 u}{\partial z^2} \tag{5}$$

where the horizontal derivatives have been neglected in comparison with the vertical derivatives on the right-hand side of equ. (5) because the length of the current is very much greater than its thickness. At the base of the fluid layer the non slip condition writes

$$u(x, 0, t) = 0 \tag{6}$$

Considering that the shear stress at the top of the current is very much less than its value within the current, it can be approximated as

$$\frac{\partial u}{\partial z}(x, h, t) = 0 \tag{7}$$

the solution of eqs. (5)-(7) is

$$u(x, z, t) = -\frac{1}{2} \frac{g}{\nu} \frac{\partial h}{\partial x} z(2h - z) \tag{8}$$

A complete determination of the unknowns u and h requires the equation of continuity which can be written here as

$$\frac{\partial h}{\partial t} + \frac{\partial}{\partial x} \left(\int_0^h u dz \right) = 0 \tag{9}$$

Substituting (8) into (9) we obtain

$$\frac{\partial h}{\partial t} - \frac{\rho g}{12\mu} \frac{\partial^2 (h^3)}{\partial x^2} = 0 \tag{10}$$

If l denotes the reservoir length, we can assume the following set of non dimensional variables:

$$(H, X, T) = \left(\frac{h}{h_0}, \frac{x}{h_0}, \frac{\rho g h_0^3}{12\mu l^2} t \right) \tag{11}$$

where subscript f denotes the wave-front, the equation of motion (10) then becomes, in the non dimensional form:

$$\frac{\partial^2 (H^3)}{\partial X^2} - \frac{\partial H}{\partial T} = 0 \tag{12}$$

Equ. (12) is similar to the equation of motion obtained by Schwarz [15] and Barthes-Biesel [16], describing the evolution of a thin liquid layer flowing down a horizontal plane when surface tension effects can be neglected.

b. Initial and boundary conditions

Using fig. 1, the fluid height at initial time is given by:

$$H(X_b(T), T) = \begin{cases} 1 & \text{for } -1 \leq X \leq 0 \\ 0 & \text{otherwise} \end{cases}$$

Furthermore, a complementary boundary condition should be imposed upstream, assuming that a short time or an asymptotic solution is sought. These boundary conditions are suggested by experimental observation. For the short time case, it is written as:

$$H(X = -L, T) = 1 \quad \text{with} \quad L = \frac{l}{h_0} \tag{14}$$

which means that only a given fluid quantity in the upper part of the reservoir is released downstream the very few moments following the dam collapse.

While for the long time case, it is written as:

$$\frac{\partial H}{\partial X}(X=-L,T)=0 \tag{15}$$

which means that there is no flow at the fixed wall; so at that site, the free surface is horizontal.

2.2 Solution

Dam-break flow belongs to the general class of gravity currents; so the solution depends on the time scale [14]. First of all, the inertial regime, characterized by a fixed height at the dam-site holds immediately after the dam collapse [3]. Then, a solution dominated by viscous effects appears and tends to an asymptotic form. The solution sought here will give the analytical expression for a short time ($T \ll 1$) and a long time ($T \gg 1$) viscous solutions, as well as the different dynamic characteristics.

Sedov [17] describes the method of investigating similar solutions of equ. (12) by means of a phase plane formalism. In fact, this equation of motion can be tackled by assuming a solution of the form

$$H(X,T)=\Omega(T)\Psi(\lambda) \text{ where } \lambda=\frac{X-\phi(T)}{P(T)} \tag{16}$$

Let $X_b(T)$ denote the front of the back wave and $X_f(T)$ the front of the positive wave. If T_c denotes the time where the back wave front reaches the rear wall, the short time regime corresponds to a viscous solution such that $T \leq T_c$. While, for larger time, H is everywhere less than 1. So, a solution should be sought such that

$$H(X_b(T),T)=\begin{cases} 1 & \text{if } T \leq T_c \\ H(-1,T) & \text{if } T \geq T_c \end{cases}$$

$$X_b(T)=\begin{cases} X_b(T) & \text{if } T \leq T_c \\ -1 & \text{if } T \geq T_c \end{cases} \tag{18}$$

Two regimes can now be identified, which correspond to two different physical mechanisms of reservoir emptying. The

short time solution is such that far downstream from the dam, the fluid seems to be at rest at a depth h_0 , so that the reservoir's length l_0 has no effect on this flow regime, while for the long time solution, the flow only retains the initial (non dimensional) volume of the reservoir $V=1L$ and not the details of its initial geometry.

a. Short time solution

The information affects the fluid contained between $X_f(T)$ and $X_b(T)$, this suggests to take

$$P(T)=X_f(T)-X_b(T), \phi(T)=X_b(T) \tag{19}$$

Introducing eqs. (13)-(15) in the equation of motion (9), we get

$$-\frac{d}{d\lambda}\left[\frac{d\Psi^4}{d\lambda}\right]+P'P\lambda\frac{d\Psi}{d\lambda}+X_b'P\frac{d\Psi}{d\lambda}=0 \tag{20}$$

Next, a condition of no flow rate must be imposed at the rear wall and at the front of positive wave

$$\frac{d^2(\Psi^4)}{d\lambda^2}=0 \text{ for } \lambda=0 \text{ and } \lambda=1 \tag{21}$$

Applying then the principle of conservation of the mass on the fluid flowing in the channel

$$\int_{X_b}^{X_f} HdX = -X_b \tag{22}$$

we can easily verify that a self-similar solution to eqs. (20)-(22) can be written

$$X_b(T)=-\gamma_0[2\gamma_1]^{1/2}T^{1/2} \tag{23}$$

$$X_{fs}(T)=(1-\gamma_0)[2\gamma_1]^{1/2}T^{1/2} \tag{24}$$

provided that the following functions:

$$\left(-\frac{X_b}{P}\right), P'P^m \text{ and } X_bP^m \text{ be constant} \tag{29}$$

respectively noted $\gamma_0, \gamma_1, (-\gamma_2)$ with $\gamma_2 = \gamma_0\gamma_1$ and which will be determined later. In equ. (24), the subscript s refers to the short time regime. Critical time T_c is obtained for $X_b = -1$ in equ. (23), there comes

$$T_c = \frac{1}{2\gamma_1\gamma_0^2} \tag{21}$$

While, using equ. (24), we see that at critical time, the abscissa of the front of the positive wave is

$$X_f(T_c) = \frac{1-\gamma_0}{\gamma_0} \tag{26}$$

Moreover, at dam position ($X = 0$), we have $\lambda = \gamma_0$, so the stage is constant in time with value

$$H_d = \Psi(\gamma_0) \tag{27}$$

b. Long time solution

At $T = T_c$, the front of the negative wave reaches the rear wall ($X_b = -1$), so for the long time solution, we can take

$$\psi(T) = -1 \text{ and } P(T) = X_f + 1 \tag{28}$$

Then, introducing equ. (28) in the equation of motion (12), we get

$$-\frac{d}{d\lambda} \left[\frac{d\Psi^4}{d\lambda} \right] + \frac{\Omega'P^2}{\Omega^4} \Psi - \frac{P'P}{\Omega^3} \lambda \frac{d\Psi}{d\lambda} = 0 \tag{29}$$

Then, a condition of no flow rate must be imposed at the front of positive wave

$$\left[\frac{d}{d\lambda} \left[\frac{d\Psi^4}{d\lambda} \right] \right]_{\lambda=1} = 0 \tag{30}$$

Applying then the principle of conservation of the mass on the fluid flowing in the channel

$$\int_{-1}^{X_f} H dX = 1 \tag{31}$$

we can easily verify that a self-similar solution to eqs. (29)-(30) can be written

$$X_{f_{il}}(T) = \gamma \left[(T - T_c) + \left(\frac{X_f(T_c) + 1}{\gamma} \right)^5 \right]^{1/5} - 1$$

provided that the following functions:

$$1/\Omega P, P'P/\Omega^3 \text{ and } \left(-\frac{\Omega'P^2}{\Omega^4} \right) \text{ be constant}$$

respectively noted γ_3 , γ_4 and γ_5 and which will be determined later. In equ. (32), the subscript l refers to the long time regime. Then, equ. (29) becomes

$$-\frac{d}{d\lambda} \left[\left[\frac{d(\Psi^4)}{d\lambda} \right] \right] + \gamma_4 \Psi + \gamma_4 \lambda \frac{d\Psi}{d\lambda} = 0 \tag{33}$$

which can take the form

$$-\frac{d}{d\lambda} \left[\frac{d\Psi^4}{d\lambda} \right] + \gamma_4 \frac{d(\lambda\Psi)}{d\lambda} = 0 \tag{34}$$

After a straightforward analytical calculation, a solution of eq. (34) is found with the form

$$\Psi(\lambda) = (\gamma_4)^{1/3} \left[\frac{3}{8} \right]^{1/3} [1 - \lambda^2]^{1/3} \tag{35}$$

The constants of integration γ_i 's are determined using the boundary and initial conditions. We find:

$$\gamma_0 = \gamma_3 = \alpha \text{ with } \alpha = \int_0^1 [1 - \lambda^2]^{1/3} d\lambda \text{ and } \gamma_4 = \left[\frac{8}{3} \right]$$

$$\gamma_1 = \beta = \frac{\left| \frac{d}{d\lambda} \left[\frac{d[1 - \lambda^2]^{4/3}}{d\lambda} \right] \right|_{\lambda=\alpha}}{\int_{\alpha}^1 [1 - \lambda^2]^{1/3} d\lambda} \tag{36}$$

2.3 Results

All the results shown here were obtained either by computing the analytical solution or numerically [12]. Both methods provided quite identical values for all investigated flow characteristics.

a. Free surface profile

The free surface profile is presented in fig.2. A large time after dam collapse, it completely differs from Ritter's solution, i.e. when the fluid is water, computed using eqs.(1)-(2) which is concave. This shows that the convex shape of free surface profile for viscous dam-break flow is intrinsic to the equations of motion governing the problem.

Furthermore, a complete description of the flow should include surface tension, introducing a complementary term in the equation of motion, say

$$\frac{\partial H}{\partial T} = 4 \frac{\partial}{\partial X} \left[H^3 \frac{\partial H}{\partial X} - \frac{1}{B} \frac{\partial^3 H}{\partial X^3} \right] \tag{37}$$

where B denotes the Bond number, defined as $B = \frac{\rho g L^2}{\sigma}$ and σ the fluid surface tension. Computation of equ. (37) was carried out using the procedure described in previous section for assigned glucose syrup concentration in water. Fluid physical properties (density, viscosity and surface tension) were taken in [21]. For similar flow configuration, results were quite identical to those obtained from equ. (38), i.e. when surface tension is neglected. In fact, surface tension would affect viscous dam-break flow, only in film lubrication conditions [15].

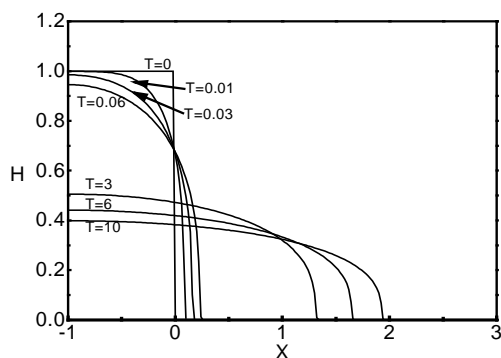


Figure 2: Time variation of free surface profile

b. Fluid height

Fig.2 also shows that during a very short while after dam collapse (short time solution), the flow height remains constant at dam site, with

$$H_d(X=0,T) \approx 0.684 \tag{38}$$

The viscous solution is characterized by a decreasing of the fluid height at dam site. At a given location inside the reservoir, time variation of the fluid height is shown in fig. 3 which indicates that the fluid height collapses for stations close to dam site followed by a smoother decrease for all upstream stations. While at given downstream station, flow height increases abruptly at first stage, then smoothly to a maximum value and finally decreases as shown in fig. 4

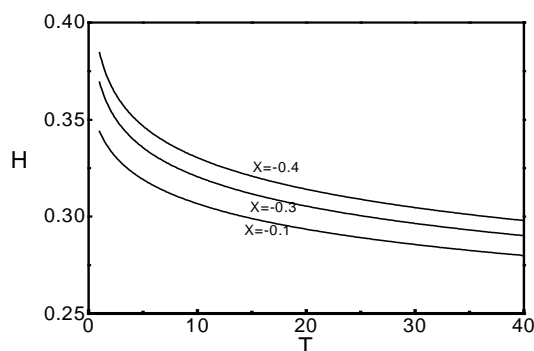


Figure 3: Typical time variation of fluid height at upstream stations

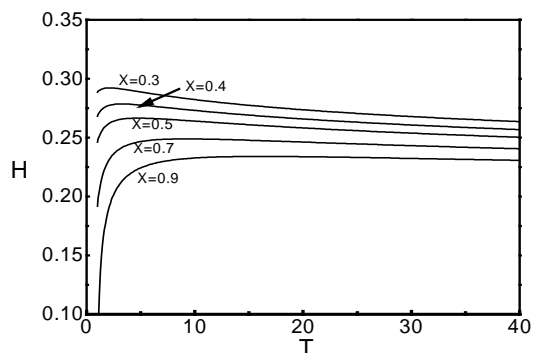


Figure 4: Typical time variation of fluid height at downstream stations

c. Maximum heights

To localize the maximum height at given down scenario described in Fig. 4 shows that

$$\frac{\partial H(X,T)}{\partial T} = 0 \tag{39}$$

While in the long time regime, we have

$$\frac{\partial H}{\partial T} = - \left[\frac{(X_f + 1)'}{\alpha_m (X_f + 1)^2} \right] (\Psi + \lambda \Psi') \tag{40}$$

So

$$\Psi + \lambda \Psi' = 0 \tag{41}$$

which gives

$$\lambda = \left(\frac{3}{5}\right)^{\frac{1}{2}} \tag{42}$$

Introducing this solution in equ. (35), the maximum height at given downstream station X is then found as

$$H_{\max}(X) = \left(\frac{2}{5}\right)^{\frac{1}{3}} \left(\frac{3}{5}\right)^{\frac{1}{2}} \frac{1}{\alpha} \frac{1}{(X+1)} \quad (43)$$

The corresponding graph (hyperbola) is shown on Fig. 5

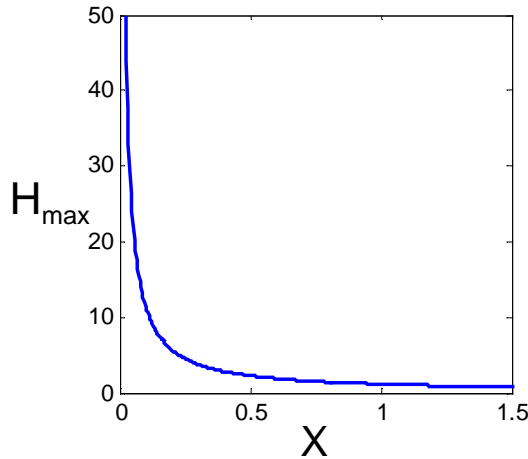


Figure 5: Variation of the maximum height at given station, vs the corresponding abscissa

and it occurs at time T_{\max} such that

$$T_{\max}(X) = \frac{1}{\gamma^5} \left(\frac{5}{3}\right)^{\frac{5}{2}} (X+1)^5 + T_c - \left(\frac{1}{\gamma \alpha}\right)^5 \quad (44)$$

whose graph is shown on Fig. 6

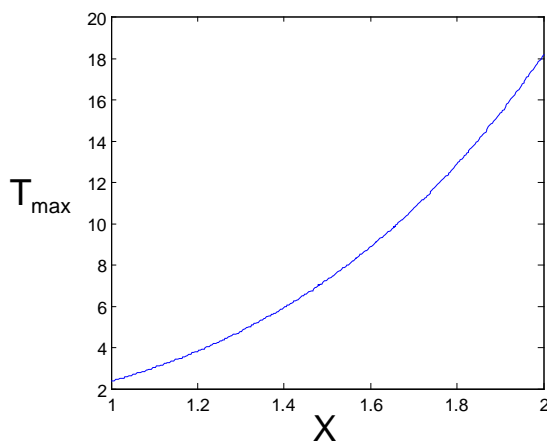


Figure 6: Variation of the time of occurrence of maximum height for given abscissa

d. Front wave position

Time evolution of the front of the positive wave is presented in fig.7. It can be obtained either numerically [12] or

analytically using equ. (20). This graph agrees with the experimental result obtained by Nsom [13] who found the following scaling law in this regime

$$X_f \propto T^{1/2} \quad (45)$$

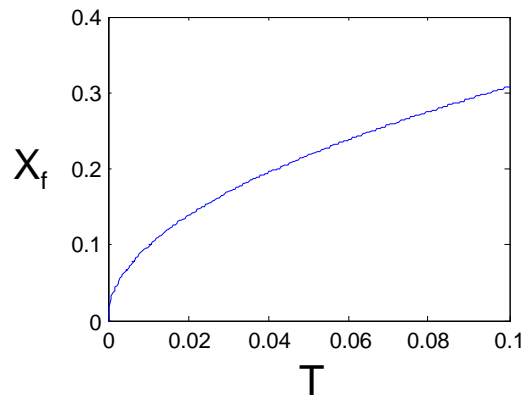


Figure 7: Evolution of the front of the positive wave front in short time viscous regime

In the same flow regime, the front of the negative wave, obtained numerically or analytically using equ. (23) is shown on fig. 8. It can be observed that $X_b(T)$ decreases vs time with a slope itself decreasing in the time.

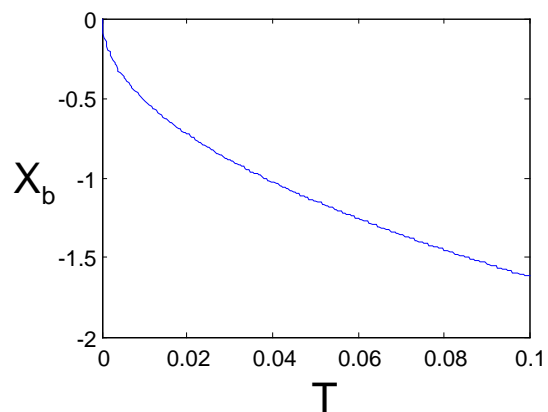


Figure 8: Evolution of the front of the negative wave front in long time viscous regime

While for long time flow regime, the graph of the equation of motion of the front wave is shown on fig. 9. It can be obtained numerically [12] or analytically using equ. (32) and this result agrees with the

experimental result obtained by Nsom [13] who found the following scaling law in this regime

$$X_f \propto T^{1/5} \tag{46}$$

In these experiments, the author performed dam-break tests using well characterized water-glucose syrup solutions.

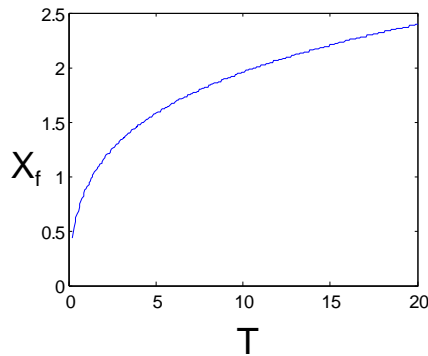


Figure 8: Evolution of the front of the positive wave front in long time viscous regime

Generally, in the literature, theoretical studies focus on the long time solution also called asymptotic solution and the scaling law obtained is of the form of equ.(44). The originality of the present paper is to have pointed out, analytically and numerically the previous two viscous flow regimes and to characterize them.

e. Front wave velocity

The wave front velocity is obtained from the time derivation of $X_f(T)$. It can be calculated analytically by a straightforward use of the corresponding equation of motion, obtained in section 2. While the numerical method consists in the following centred second order scheme :

$$U_f\left(T+\frac{\Delta T}{2}\right) = \frac{X_w(T+\Delta T) - X_f(T)}{\Delta T} + O(\Delta T^2)$$

where U_f denotes the front velocity and subscript w is used for b , fs and fl when referring to the front of back wave or positive wave in the short time regime and in the long time regime, respectively. The results obtained using both methods are concordant.

These graphs clearly show that for each wave, the velocity is time decreasing and tends to an asymptotic value which for the positive wave characterizes a 1D film lubrication.

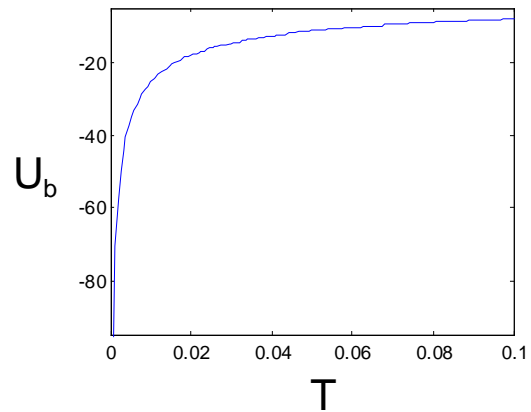


Figure 9: Time variation of the velocity of the back wave

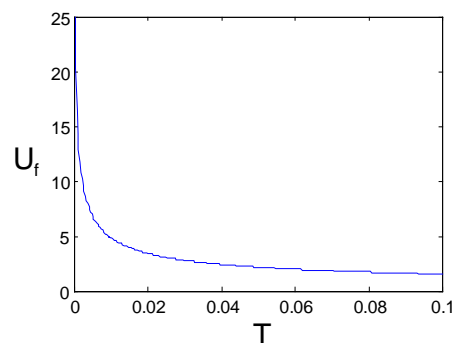


Figure 10: Time variation of the velocity of the positive wave in the short time regime

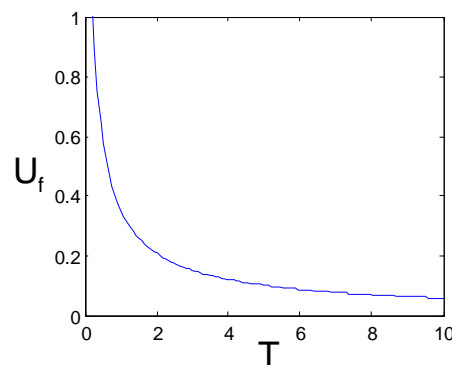


Figure 11: Time variation of the velocity of the positive wave in the long time regime

3 The dam-break flow of clayous mud

3.1 Rheology

Muddy flash floods and debris flows are mass movements mobilizing large quantities of coarse grains suspended in a colloidal dispersion (clay-water mixture). They can be modelled by means of Rheology. Constitutive equations are needed which relate the various mathematical relationships with respect to stresses in the flowing unloaded mud to the rate of deformation, as well as with respect to the other relevant microscopic or macroscopic parameters. For the last 50 years, such equations have been suggested for equivalent monophasic media by: Herschel and Bulkley [22], Bagnold [23], Takahashi [24], Savage and Hutter [25], among others. Nevertheless, the Reiner-Rivlin form of stress proves to be useful as a monophasic model for a complex fluid mixture, as noticed in the ASCE 1997 Conference on Debris Flow Hazards Mitigation. Herschel-Bulkley constitutive equations as initially developed by Bingham [26] have been worked on for some time, with application to rheometry data fitting [27], and to hydraulics flow modelling [28] and they have been shown to accurately describe the rheological behaviour of natural unloaded mud (e.g. [29]). The Herschel-Bulkley model is characterized by two main properties: plasticity (described by the yield stress) and shear-thinning (described by fluid consistency and power-law index). The rheological modelling consists in considering the studied two-phase fluid as a single phase complex material gifted with a stress-rate of strain equation and which obeys the equations of conservation of mass and momentum.

Since the flow is isochoric, it is governed by the conservation of mass and momentum equations, respectively, in the following form:

$$\text{div} \vec{u} = 0 \quad (47)$$

$$\rho \frac{d\vec{u}}{dt} = \rho \vec{g} - \vec{\nabla} p + \text{div} [2\eta D(\vec{u})] \quad (48)$$

where \vec{u} is the velocity field, p the pressure field, ρ the fluid density, and \vec{g} the gravity. We assume that a relationship exists between the stress and the strain rate. Nguyen and Boger [30] showed that a debris flow conforms to a viscoplastic behavior scheme governed by the Herschel-Bulkley rheological equation. Doraiswamy et al. [31] among others, confirmed this result. The Herschel-Bulkley model is written as follows :

$$\underline{\tau} = 2\eta D(\vec{u}) \quad \text{if} \quad -\tau_{II} > \tau_0^2 \quad (49)$$

$$D(\vec{u}) = 0 \quad \text{if} \quad -\tau_{II} \leq \tau_0^2 \quad (50)$$

where $\underline{\tau}$ denotes the stress tensor, $D(\vec{u})$ the strain-rate tensor, and η the apparent viscosity, defined as :

$$\eta = k(-4D_{II})^{\frac{n-1}{2}} + \frac{\tau_0}{(-4D_{II})^{\frac{1}{2}}} \quad (51)$$

where k is the fluid consistency, τ_0 its yield stress and n the power-law index.

At this point, some assumptions can be made to simplify the equations [32]. However, Piau [33] formulated a more general approach, without resorting to such assumptions. In this paper, using similar reasoning and retaining the three rheological parameters (τ_0, k, n) , we extend Piau's study [33] and we derive an operational equation of motion which refers to usual simplified models (Newtonian, power-law and Bingham) for given values of the parameters. To completely describe the flow field, the initial and boundary conditions based on the specific configuration of the studied flow are to be taken into account. In this paper, the dam-break flow is considered. It constitutes a given scenario covering the initiation of debris flows (e.g. Malpasset, France in 1959). A non dimensional equation of motion is built and solved analytically. For validation, the obtained solution will be compared to the limiting cases of power-law model and Newtonian model as well, existing in the literature. As generally encountered in nature, the

flow is assumed two-dimensional in the (x,y) plane of an orthonormal coordinate system (O,x,y,z) , in a space domain much longer (x -direction) than thick (y -direction). The following characteristic quantities can be defined: velocity U_0 , height H , length L and a small parameter ϵ given by: $\epsilon = \frac{H}{L}$, the following set of normalized variables are defined:

$$X = \frac{x}{L}; Y = \frac{y}{\epsilon L}; T = \frac{U_0}{L}t; U = \frac{u}{U_0} \quad (52)$$

$$V = \frac{v}{\epsilon U_0}; P = \frac{p}{\rho U_0^2}; \xi = \frac{\epsilon L}{U_0}(-4D_{II})^{1/2} \quad (53)$$

The equations of motion obtained in a non-dimensional form contain a Reynolds, a Froude and an Oldroyd numbers respectively defined by (see [33]):

$$Re = \frac{\rho U_0^{2-n} (\epsilon L)^n}{k} \epsilon; Fr = \frac{U_0^2}{g \epsilon L} \quad (54)$$

$$Od = \frac{s \epsilon}{k} \left(\frac{L \epsilon}{U_0} \right)^n \quad (55)$$

Assuming $\epsilon \ll 1$ and $Re \geq 1$, eq.(82) takes the form

$$\frac{\partial P}{\partial Y} = \frac{-1}{\epsilon Fr^2} \cos \alpha + \frac{\epsilon Od}{Re} \left\{ \xi^{-1} (U_{,Y} + \epsilon^2 V_{,X}) \right\}_{,X} + 2 \left\{ \xi^{-1} V_{,Y} \right\}_{,Y} \quad (56)$$

Then, by neglecting the X-variation of the shear stress versus the Y-variation of the Y normal component of the yield stress, $(\tau_{YY}^s \gg \tau_{XY,X})$, we obtain a quadrature of eq. (91):

$$p = \rho g \cos \alpha \cdot (h-y) + \tau_{YY}^s \quad (57)$$

where

$$\tau_{YY}^s = \frac{2 \tau_0 v_{,Y}}{\left[4u_{,X}^2 + (u_{,Y} + v_{,X})^2 \right]^{1/2}} \quad (58)$$

while eq. (83) in a dimensional form, reduces to

$$\rho \frac{du}{dt} + \rho g \cos \alpha \frac{dh}{dx} + \tau_{yy,x}^s = \rho g \sin \alpha + \tau_{xx,x}^s + \tau_{xy,y}^s$$

where

$$\tau_{yy}^s = 2 \tau_0 \left[4u_{,X}^2 + (u_{,Y} + v_{,X})^2 \right]^{1/2} \cdot v_{,Y} \quad (59)$$

$$\tau_{xx}^s = 2 \tau_0 \left[4u_{,X}^2 + (u_{,Y} + v_{,X})^2 \right]^{1/2} \cdot u_{,X} \quad (60)$$

$$\tau_{xy}^s = \tau_0 \epsilon \left[4u_{,X}^2 + (u_{,Y} + v_{,X})^2 \right]^{1/2} \cdot (u_{,Y} + v_{,X}) \quad (61)$$

Neglecting inertia and defining the form-parameter ϕ by:

$$\phi = \frac{1}{\tau_0 h_{,x} \operatorname{sgn} h_{,x}} \int_0^h (\tau_{yy}^s - \tau_{xx}^s) dy \quad (62)$$

where $\operatorname{sgn}(\cdot)$ denotes the sign-function :

$$\begin{aligned} \operatorname{sgn}(x) &= 1 \quad \text{if } x > 0 \\ &= 0 \quad \text{if } x = 0 \quad \text{and} \\ &= -1 \quad \text{si } x < 0 \end{aligned} \quad (63)$$

and the friction slope j is defined from the wall-friction τ_p by :

$$j = \frac{\tau_p}{\rho g h} \quad \text{with} \quad \tau_p(x) = \tau_{xy}(x,0) \quad (64)$$

A quadrature of Equation (94) from $y=0$ to $y=h$, gives:

$$\left(g \cos \alpha - \frac{\tau_0}{\rho h} \phi \right) \frac{dh}{dx} = g (\sin \alpha - j) \quad (65)$$

3.2 Velocity profile and flow rate

Consider a Herschel-Bulkley shear flow model in the (x,y) plane. Its rheological equation is written as:

$$\tau_{xy}(x,y) = \tau_0 + k |u_{,y}|^n \quad (66)$$

$$\tau_{xx}(x,y) = \tau_{yy}(x,y) = 0 \quad (67)$$

$$x \in I; \quad y \in [0, h(x)] \quad (68)$$

I being a given space interval. Its equation of motion is expressed by :

$$\operatorname{div} \tau = \nabla p - \rho g \quad (69)$$

and its x-projection after integration from $y=0$ to $y=h$ yields

$$\tau_{xy}(x,y) = \left[\frac{dp(x)}{dx} - \rho g \sin \alpha \right] (h(x) - y) \quad (70)$$

If $a(x)$ denotes the pressure loss, then:

$$a(x) = - \left[p(x)_{,x} - \rho g \sin \alpha \right] \quad (71)$$

We can see that $a(x)$ is positive for any x abscissa in the flow domain, since $(-p(x))_{,x} > 0$ and $\sin \alpha > 0$, so that

$$\tau_{xy}(x,y) = a(x) [h(x) - y] > \tau_0 \quad (72)$$

and

$$y < h(x) - \frac{\tau_0}{a(x)} \quad (73)$$

Introducing the critical height and the wall friction defined, respectively, by:

$$h_c(x) = h(x) - \frac{\tau_0}{a(x)} ; \tau_p(x) = \tau_{xy}(x, 0) \quad (74)$$

we obtain the following expressions for the friction slope:

$$j(x) = \frac{a(x)}{\rho g} \quad (75)$$

Then, using the behavior law (eq. (67)):

$$k \left(|u_{,y}|^n \right)_{,y} = -a(x) \quad (76)$$

After an integration between $y=0$ and $y=h_c(x)$ and substituting $m = \frac{1}{n}$:

$$u(x, y) = \frac{1}{m+2} \left| \frac{a(x)}{k} \right|^m \left[|h_c^{m+1}(x) - |h_c(x) - y|^{m+1}| \right] \quad \text{if} \\ 0 \leq y \leq h_c(x), \quad \forall x \in I \quad (77)$$

$$u(x, y) = \frac{1}{m+2} \left| \frac{a(x)}{k} \right|^m h_c^{m+1}(x) \quad \text{if} \quad h_c(x) \leq y \leq h, \\ \forall x \in I \quad (78)$$

The flow rate defined by:

$$Q(x) = \int_0^{h(x)} u(x, y) dy \quad (79)$$

is then derived by integration of Equations (113) and (114) in the form:

$$Q(x) = \frac{1}{m+2} \left| \frac{a(x)}{k} \right|^m \left| h(x) - \frac{\tau_0}{a(x)} \right|^{m+1} \left(h(x) + \frac{\tau_0}{(m+1)a(x)} \right) \quad (80)$$

3.3 Equation of motion

Substituting eq. (75) for Equation (65) yields:

$$a(x) = \rho g \left[\sin \alpha - \left(\cos \alpha - \frac{\phi \tau_0}{\rho g h(x)} \right) \frac{\partial h(x)}{\partial x} \right] \quad (81)$$

Substituting this expression of $a(x)$ for the flow-rate (eq. (80)), we obtain

$$\frac{\partial h}{\partial t} + \frac{\partial (h U_m)}{\partial x} = 0 \quad (82)$$

where $U_m = \frac{Q}{h}$ denotes the average velocity. Then :

$$\frac{\partial h}{\partial t} + \frac{1}{(m+2)k} \frac{\partial}{\partial x} \left[a^m \left(h - \frac{\tau_0}{a} \right)^{m+1} \left(h + \frac{\tau_0}{(m+1)a} \right) \right] = 0 \quad (83)$$

Special cases

- Newtonian fluid in horizontal channel : $\alpha=0 ; \tau_0=0 ; m=1$

$$Q = -\frac{\rho g}{3k} h^3 \frac{\partial h}{\partial x} \quad (84)$$

- Power-law fluid horizontal channel : $\alpha=0 ; \tau_0=0$

$$a = -\rho g \frac{\partial h}{\partial x} \quad (85)$$

- Herschel-Bulkley fluid in horizontal channel : $\alpha=0$

$$a = -\rho g \left(1 - \frac{\phi \tau_0}{\rho g h} \right) \frac{\partial h}{\partial x} \quad (86)$$

Among others, the special cases of Newtonian fluid was considered by Cavaillé and Fortier [34] and by Huppert [35]; while the power law fluid was considered by Gratton & Minotti [36], and by Piau & Debiane [37], as well. Their results are easily recovered by using appropriate corresponding values of the rheological parameters in the present solution.

4 Modelling muddy flash floods

The equations of conservation of mass and momentum (47)-(48) can be rewritten in the following non-dimensional form [33], when the viscous terms are much smaller than the inertial ones:

$$U_{,t} + \beta U U_{,x} + \left(g \cos(\alpha) + \frac{s\Phi}{\rho h} \operatorname{sgn} h_{,x} \right) h_{,x} = g(\sin \alpha - J) \quad (87)$$

$$h_{,t} + U h_{,x} + h U_{,x} = 0 \quad (88)$$

$$U_{,x} dx + U_{,t} dt = dU ; h_{,x} dx + h_{,t} dt = dh \quad (89)$$

where α is the sloping angle of the (Oxz) plane to the horizontal, β the average form coefficient, Φ the exact form coefficient and J the friction slope. The set of equations (87)-(89) constitute the mathematical model of the motion of a

muddy flash flood, i.e. the inertial dam-break one dimensional flow of a Herschel-Bulkley fluid along a (Oxz) plane sloping with an angle α to the horizontal. The friction slope J appearing in this solution must be determined. Its expression is known only for the power-law fluid [37] but not for the Herschel-Bulkley fluid.

4.1 The friction slope

Whatever the rheological equation of the fluid is, the friction slope is defined as

$J = -\frac{1}{\rho g} \frac{\partial \tau}{\partial y}$ so, after one quadrature, we get:

$$\tau = -\rho g J (y-h) \tag{90}$$

The Herschel-Bulkley fluid is characterized by two zones [28]: a rigid zone where the shear stress is less than the yield value, and which is thus

characterized by $y \geq h - \frac{s}{\rho g J}$ and a sheared zone where the shear stress is greater than the yield value, and which is thus characterized by

$$k \frac{\partial \left(\dot{\gamma} \right)^n}{\partial y} = -\rho g J \tag{91}$$

The two zones are separated by the yield surface with height $y_0 = h - \frac{s}{\rho g J}$. Both the rigid zone and the yield surface undergo a rigid body motion, while the shearing rate is obtained after an integration of equ. (14) from y_0 to y as:

$$\frac{\partial u}{\partial y} = \left(\frac{\rho g J}{k} \right)^{\frac{1}{n}} (y_0 - y)^{\frac{1}{n}} \tag{92}$$

Integrating equ. (92) from 0 to y and putting $m = \frac{1}{n}$, we can write the velocity profile in a given section in the form:

$$u = u_{\max} \left[1 - \left(1 - \frac{y}{y_0} \right)^{m+1} \right] \quad \text{for } y \leq y_0 \tag{93}$$

$$u = u_{\max} \quad \text{for } y \geq y_0 \tag{94}$$

where

$$u_{\max} = \frac{1}{m+1} \left(\frac{\rho g J}{k} \right)^m y_0^{m+1} \tag{95}$$

From this solution, the flow rate and the average velocity are derived respectively as:

$$Q = \int_0^{y_0} u \cdot dy + \int_{y_0}^h u \cdot dy = \frac{u_{\max}}{m+2} [(m+2)h - y_0] \tag{96}$$

$$U = \frac{Q}{h} = \frac{\left(\frac{\rho g J}{k} \right)^m h^{m+1} \left(1 - \frac{s}{\rho g h J} \right)^{m+1}}{(m+2)(m+1)} \left((m+1) + \frac{s}{\rho g h J} \right) \tag{97}$$

The expression of the friction slope given by Piau and Debiante [37] for a power-law fluid is recovered by putting $s = 0$ in equ. (133), i.e.:

$$J = \frac{k}{\rho g} \left(\frac{m+2}{h^{m+1}} \right)^{\frac{1}{m}} U^{\frac{1}{m}} \tag{98}$$

and the well-known following formula for the Newtonian fluid: $s = 0$, $m = 1$, $k = \mu$

$$J = \frac{3\mu}{\rho g h^2} U \tag{99}$$

In the general case of a Herschel-Bulkley fluid ($s \neq 0$, $m \neq 1$), it is difficult to derive an analytical expression of the friction slope from equ. (96). Meanwhile, the following approximate expression can be obtained for the limiting case of the inertial regime:

$$J = (m+2)^{\frac{1}{m}} \frac{k}{\rho g h} \left(\frac{U}{h} \right)^{\frac{1}{m}} + \frac{s}{\rho g h} \tag{100}$$

4.2 Solution

Putting $a = \left(gh \cos(\alpha) + \frac{\phi s}{\rho} \operatorname{sgn} h_x \right)^{\frac{1}{2}}$ if $h \geq \frac{-\phi s}{\rho g \cos(\alpha)} \operatorname{sgn} h_x$ (101)

$$\text{and } a = \left(-gh \cos(\alpha) - \frac{\varphi_s}{\rho} \operatorname{sgn} h_{,x} \right)^{\frac{1}{2}} \quad \text{if}$$

$$h \leq \frac{-\varphi_s}{\rho g \cos(\alpha)} \operatorname{sgn} h_{,x} \quad (102)$$

equ. (87) becomes:

$$U_{,x} + \beta U U_{,x} \mp \frac{a^2}{h} h_{,x} = g(\sin(\alpha) - J) \quad (103)$$

The solution to system (87)-(89) is obtained if its determinant is zero, which leads to:

$$\frac{dx}{dt} = U \mp a \quad (104)$$

where we took $\beta=1$, as usual in Hydraulics. The system is undetermined if any of the columns of its determinant is replaced by its right-hand side. So

$$\frac{dU}{dt} \mp \frac{a}{h} \frac{dh}{dt} = g(\sin(\alpha) - J) \quad (105)$$

Using

$$h = \frac{a^2}{g \cos(\alpha)} - \frac{\varphi_s}{\rho g \cos(\alpha)} \operatorname{sgn} h_{,x} \quad (106)$$

we get

$$\frac{dU}{dt} \mp \frac{2a^2}{a^2 - \frac{\varphi_s}{\rho} \operatorname{sgn} h_{,x}} \frac{da}{dt} = g(\sin(\alpha) - J) \quad (107)$$

To solve this differential equation, if we

put $r(a) = a \left(\frac{\rho}{\varphi_s} \right)^{\frac{1}{2}}$ and we search a function

$$f(r) \text{ such that}$$

$$\mp \frac{2r^2}{r^2 - \operatorname{sgn} h_{,x}} \frac{da}{dt} = \frac{d(\mp 2a(1 - r^{-1} f(r)))}{dt} \quad (108)$$

so, $f(r)$ is solution of:

$$\frac{-r^2 \operatorname{sgn} h_{,x}}{r^2 - \operatorname{sgn} h_{,x}} = \frac{df(r)}{dr} \quad (109)$$

Now, let $r = tg(\beta)$, the solution is obtained after a straightforward algebraic handling in the form:

$$f(r) = \arctg(r) \text{ or } f(r) = \operatorname{arccoth}(r) \quad (110)$$

according that $\operatorname{sgn} h_{,x} = -1$ or $\operatorname{sgn} h_{,x} = +1$, respectively and equation of motion (107) becomes:

$$\frac{d[U \mp 2a(1 - r^{-1} f(r))]}{dt} = 0 \quad (111)$$

It can be solved using the method of characteristics. As $h_{,x} < 0$, there comes

$$a = \left(gh - \frac{\varphi_s}{\rho} \right)^{\frac{1}{2}} \text{ and } r = a \left(\frac{\rho}{\varphi_s} \right)^{\frac{1}{2}} \quad (112)$$

Indeed, two characteristics of eq. (112) can be defined. The negative characteristic where the gradient $\frac{dx}{dt}$ is constant and equal to $U - a$ and the quantity $U - 2a(1 - r^{-1} f(r))$ remains constant. While the positive characteristic along which the gradient is constant and equal to $U + a$ and the quantity $U + 2a(1 - r^{-1} f(r))$ remains constant.

4.3.1 The law of propagation of the wave front

Consider at initial time, the negative characteristic noted C_0^- such that the fluid height is constant and equal to h_0 and the average velocity is zero. So, in the $(x-t)$ plane, its graph is a straight line with slope

$$\frac{dx}{dt} = -a_0 \text{ where } a_0 = \left(gh_0 - \frac{\varphi_s}{\rho} \right)^{\frac{1}{2}} \quad (113)$$

At time $t = \theta$, the negative characteristic C_θ^- is such that the gradient is given by

$$\frac{dx}{dt} = U(\theta) - a(\theta) \quad (114)$$

Along a positive characteristic C^+ intersecting both C_0^- and C_θ^- , the quantity $U + 2a(1 - r^{-1} f(r))$ remains constant, so

$$U + 2a(1 - r^{-1} \arctan(r)) = 2a_0(1 - r_0^{-1} \arctan(r_0))$$

where $r_0 = a_0 \left(\frac{\rho}{\phi_s} \right)^{1/2}$. Introducing equ.

(115) in equ. (114) we obtain:

$$\left(\frac{dx_b}{dt} \right)_\theta = 2a_0(1-r_0^{-1}\arctan(r_0)) - 2a(1-r^{-1}\arctan(r)) - a(\theta) \frac{x^*}{t^*} = \phi_c^{1/2} (2r_0 - 2\arctan(r_0) + 2\arctan(r) - 3r)$$

The propagation velocity of the negative wave is derived as:

$$a(\theta) = a_0, \quad \forall \theta$$

and

$$\left(\frac{dx_b}{dt} \right)_\theta = -a_0 \tag{117}$$

To find the propagation velocity of the wave front in a Newtonian fluid, it is assumed that the fluid height is zero at the front. For a viscoplastic fluid, we assume that at the front, the fluid height is $\frac{\phi_s}{(\rho g)}$ because if not, our set of equations of motion is determined and there is no wave propagation. So, with this condition, equ. (114)-(116) give:

$$\left(\frac{dx_f}{dt} \right)_\theta = 2a_0(1-r_0^{-1}\arctan(r_0)) \tag{118}$$

As the gradient along a given characteristic is constant, we can write

$$\left(\frac{dx}{dt} \right)_\theta = \frac{x}{t} \tag{119}$$

So, equ. (119) gives:

$$\frac{x}{t} = 2a_0(1-r_0^{-1}\arctan(r_0)) - 2a(1-r^{-1}\arctan(r)) - a(t) \tag{120}$$

where $r = a_0 \left(\frac{\rho}{\phi_s} \right)^{1/2}$. Adopting the following set of non dimensional variables

$$x^* = \frac{x}{H} ; \quad h^* = \frac{h}{H} ; \quad t^* = t \sqrt{\frac{g}{H}} \tag{15621}$$

where H is a reference height. If we note

$\phi_c = \frac{\phi_s}{\rho g H}$, equ. (121) becomes in non dimensional form:

$$\frac{x^*}{t^*} = \phi_c^{1/2} (2r_0 - 2\arctan(r_0) + 2\arctan(r) - 3r)$$

where

$$r = \left[\frac{h^*}{\phi_c} - 1 \right]^{1/2} ; \quad \phi_c \leq h^* \leq 1 \tag{122}$$

$$r_0 = \left[\frac{1}{\phi_c} - 1 \right]^{1/2} \tag{123}$$

and equ. (120) gives:

$$\frac{dx_b^*}{dt^*} = [1 - \phi_c]^{1/2} \tag{124}$$

$$\frac{dx_f^*}{dt^*} = 2\phi_c^{1/2} [2r_0 - \arctan(r_0)]^{1/2} \tag{125}$$

Remark that if we put $s = 0$ in eqs. (122)-(125), we recover the well-known results for the Newtonian fluid, say:

$$\frac{x^*}{t^*} = (2 - 3h^*)^{1/2} ; \quad \frac{dx_b^*}{dt^*} = 1 ; \quad \frac{dx_f^*}{dt^*} = 2 \tag{126}$$

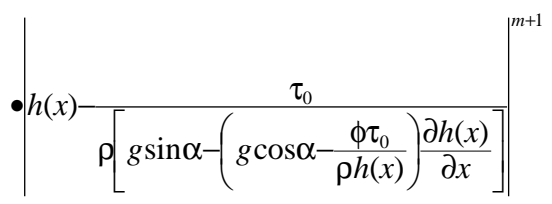
5 Modelling muddy debris flows

The general model presented in section 3 and which has been used for the muddy flash floods remains valid for muddy debris floods provided that the inertial terms be neglected against the viscous ones in the momentum balance equation. Moreover, the time scale must be much larger. As it was presented previously, the Herschel-Bulkley model is characterized by two main properties: plasticity (described by the yield stress) and shear-thinning (described by fluid consistency and power-law index). It is known that in the field, the shearing rate is often less than $100s^{-1}$ ([38]-[40]). Furthermore, Ng and Mei [41]state that at a low shear rate, the

power-law model which only takes into account the shear-thinning property of the mud [42]-[44] and neglects its plasticity is more appropriate. In specific conditions (time and position), the yield stress effects become predominant and the flow slows down until it stops.

5.1 Equation of motion

The equation of motion (83) can be expanded in the form

$$\frac{\partial h(x)}{\partial t} + \frac{1}{m+2} \left| \frac{\rho}{k} \right|^m \frac{\partial}{\partial x} \left[g \sin \alpha - \frac{\phi \tau_0}{\rho h(x)} \left| \frac{\partial h(x)}{\partial x} \right|^m \right] = 0 \quad (127)$$


Coussot and Proust [45] investigated the unconfined spreading of a rivulet of mud, obeying the Herschel-Bulkley model with a discrepancy between theory and experiment, illustrated in Fig. 6 of that paper. Wilson and Burgess [46] re-examining the problem, could explain this discrepancy but their solution appears contrary to what could be expected in some cases. In fact, the hyperbolic set of equ. (162) is very difficult to solve because of the presence of the yield surface along which the shear stress equals the yield stress. The position of the yield surface is not known a priori and has to be solved as part of the transient non linear problem. This model was used by Huang and Garcia [47] to find a matched asymptotic solution to investigate the spreading and deposit of sediment using a Herschel-Bulkley down a relatively steep slope, the solution being valid at a substantial distance downslope.

In this case, the yield stress being neglected, the flowing material is termed a power law fluid and the previous equation

of state takes the following reduced form:

$$\frac{\partial H}{\partial T} + \frac{\partial}{\partial X} \left[\frac{\partial \left(H^{(2m+2)/m} \right)}{\partial X} \right] = 0 \quad (128)$$

5.2 Analytical solution

Scaling laws governing the debris flows motion can be obtained using the method of similarity. Assume a solution of equ. (128) with the following form:

$$H(X,T) = H(X_b(T), T) X(\eta) \quad (129)$$

where

$$\eta = \frac{X - X_b(T)}{P(T)} \quad (130)$$

and

$$P(T) = X_f(T) - X_b(T) \quad (131)$$

where $X_b(T) \leq 0$ denotes the position of the front of the back wave and $X_f(T) \geq 0$ is the position of the front of the positive wave at which H vanishes.

At first stage, $X_b(T)$ decreases with time from 0 to -1 , while $H=1$. The fixed plate $X_b(T)$ is reached at time $T=T_c$. For larger time, H is everywhere less than 1. This analysis suggests to propose the following scaling laws:

$$H(X_b(T), T) = \begin{cases} 1 & \text{if } T \leq T_c \\ H(-1, T) & \text{if } T \geq T_c \end{cases} \quad (132)$$

and

$$X_b(T) = \begin{cases} X_b(\hat{t}) & \text{if } T \leq T_c \\ -1 & \text{if } T \geq T_c \end{cases} \quad (133)$$

Two regimes have been identified which correspond to different physical mechanisms of reservoir emptying and are

similar to the short time viscous regime and long time regime characterized in the Newtonian model. Let $X(\eta)$ be noted $X_1(\eta)$ in the first regime and $X_2(\eta)$ in the second regime. Since the totale fluid volume equals 1 at $T=0$ and is conserved, we can write for $T \leq T_c$

$$-\frac{d}{d\eta} \left[\left(\frac{d}{d\eta} \left[X_1^{(2m+2)/m} \right] \right)^m \right] + b_m \eta \frac{d}{d\eta} [X_1] + F_1(\eta) = 0$$

where

$$F_1(\eta) = b_m a_m \frac{d}{d\eta} [X_1] \tag{135}$$

and for $T \geq T_c$

$$-\frac{d}{d\eta} \left[\left(\frac{d}{d\eta} \left[X_2^{(2m+2)/m} \right] \right)^m \right] + d_m X_2 + d_m \eta \frac{d}{d\eta} [X_2] = 0 \tag{136}$$

where a_m, b_m and c_m are constants to be determined.

The conservation of the fluid volume at time $T=T_c$ gives:

$$a_m = \int_0^1 X_1(\eta) d\eta = \int_0^1 X_2(\eta) d\eta \tag{137}$$

The boundary conditions being:

$$X_1(0) = X_2(0) = 1 ; X_1(1) = X_2(1) = 0 \tag{138}$$

and the flow rate at the $X=X_f(T)$ being equal to:

$$\frac{d}{d\eta} \left[X_2^{(2m+2)/m} \right]_{\eta=1} = \frac{d}{d\eta} \left[X_1^{(2m+2)/m} \right]_{\eta=1} = 0 \tag{139}$$

hence, the solution of eq. (134) and satisfying the condition of continuity of H at $T=T_c$ and the boundary condition (138) writes:

$$X_2(\eta) = \left(1 - \eta^{(1+m)/m} \right)^{m/(2m+1)} \tag{140}$$

The similarity solution for the position of the wave front writes, for the back wave

$$X_b(T) = -a_m [(m+1)b_m]^{1/(m+1)} T^{1/(m+1)} \tag{141}$$

and for the positive wave:

$$X_f(T) = (1 - a_m [(m+1)b_m]^{1/(m+1)}) \text{ if } T \leq T_c \tag{142}$$

while, if $T > T_c$

$$X_f = c_m \left[(T - T_c) + \left(\frac{1}{a_m c_m} \right)^{(3m+2)} \right]^{1/(3m+2)} - 1 \tag{143}$$

where c_m is the following constant:

$$c_m = \left[\frac{(3m+2) \left(\frac{2(m+1)^2}{m(2m+1)} \right)^m}{a_m^{(2m+1)}} \right]^{1/(3m+2)} \tag{144}$$

while the reservoir height at $X=-1$ is given by:

$$H(-1, T) = \begin{cases} 1 & \text{if } T \leq T_c \\ \frac{1}{a_m [X_f(T) + 1]} & \text{if } T > T_c \end{cases}$$

with

$$T_c = \frac{1}{(m+1)b_m a_m^{(m+1)}} ; X_f(T_c) = \frac{1 - a_m}{a_m}$$

In the first regime, the height at the dam position ($X=0$) remains constant and equal to $X_1(a_m)$, while the constants d_m and a_m are given by:

$$d_m = \left[\frac{2(m+1)^2}{m(2m+1)} \right]^m \tag{146}$$

$$a_m = \int_0^1 \left[1 - \eta^{(1+m)/m} \right]^{m/(2m+1)} d\eta \tag{147}$$

The continuity of the flow at $T=T_c$ and $X=0$ provides the following expression for the constant b_m :

$$b_m = \frac{\left[\frac{2(m+1)^2}{(2m+1)m} \right]^m a_m \left[1 - a_m^{(1+m)/m} \right]^{m/(2m+1)}}{\int_{a_m}^1 \left[1 - \eta^{(1+m)/m} \right]^{m/(2m+1)} d\eta} \quad (148)$$

Some related quantities can be calculated from this solution. For an observer located at $X > 0$, the height is maximum at time $T = T_{max}$, which satisfies $H(X, T)_{,T} = 0$.

For $T \leq T_c$, the only solution is $X = 0$. And when $T > T_c$, this condition leads to

$$\eta = \left[\frac{2m+1}{3m+2} \right]^{m/(m+1)} \quad (149)$$

so,

$$T_{max}(X) = A(X+1)^{(3m+2)} + T_c - \left(\frac{1}{a_m c_m} \right)^{3m+2}$$

where

$$A = \frac{1}{c_m^{(3m+2)}} \left[\frac{3m+2}{2m+1} \right]^{m(3m+2)/m+1} \quad (150)$$

Moreover, at time $T = T_{max}(X)$, the front position is given by:

$$X_f(T_{max}) = (X+1) \left[\frac{3m+2}{2m+1} \right]^{m/(m+1)} - 1 \quad (151)$$

and the corresponding height is given by:

$$H_{max}(X) = \frac{B}{a_m(X+1)} \quad (152)$$

where

$$B = \left[\frac{m+1}{3m+2} \right]^{m/(2m+1)} \left[\frac{2m+1}{3m+2} \right]^{m/(m+1)} \quad (153)$$

5.3 Numerical solution

a. Discretization

The problem to solve numerically is the same which has been solved analytically in the previous section by equ. (128). To build a numerical procedure, it is necessary to define the channel total length l_t . The non dimensional extreme (downwards)

abscissa is $L_e = \frac{l_t - l}{h_0}$. This point is so far from dam site, that the flow is supposed to never reach it during a given experiment (1D assumption), with total duration τ . This assumption constitutes the following complementary boundary condition:

$$H(X_e, T) = 0 \quad \forall T \geq 0 \quad (154)$$

This problem is solved by an explicit finite difference method. For this, the function $H(X, T)$ is computed in the set $[-L, L_e] \times [0, \tau]$, itself discretized in a finite number of identical small rectangles with sides ΔT and ΔX .

The equation will be approximated at grid points located at the following coordinates in the $[-L, L_e] \times [0, \tau]$ set:

$$\begin{aligned} (X_i, T_j) &= (-L + i \cdot \Delta X, j \cdot \Delta T) \\ i &\in \left[0, \frac{-L + L_e}{\Delta X} \right], \quad j \in \left[0, \frac{\tau}{\Delta T} \right] \end{aligned} \quad (155)$$

b. Algorithms

Using Taylor's formula, the derivative of the unknown function can be given by:

$$\begin{aligned} \frac{\partial H}{\partial T}(X, T) &= \frac{H(X, T + \Delta T) - H(X, T)}{\Delta T} - A, \\ A &= \sum_{n \geq 2} \frac{\Delta T^{n-1}}{n!} \frac{\partial^n}{\partial T^n} H(X, T) \end{aligned} \quad (156)$$

Also, Taylor's formula can be used to write the non linear term in eq.(26):

$$\begin{aligned} \frac{\partial^2 (H^4)}{\partial X^2}(X, T) &= B - \sum_{p \geq 2} \frac{\Delta X^{2(p-1)}}{(2p)!} \frac{\partial^{2p} (H^4)}{\partial X^{2p}}(X, T) \\ B &= \frac{[H(X + \Delta X, T)]^4 + [H(X - \Delta X, T)]^4 - 2[H(X, T)]^4}{\Delta X^2} \end{aligned} \quad (157)$$

Introducing eq.(193) and eq.(194) in eq.(163) gives

$$\frac{H(X, T + \Delta T) - H(X, T)}{\Delta T} = C_1 + C_2 + R_{\Delta X, \Delta T}(X, T) \quad (158)$$

$$C_1 = \left(\frac{2m+2}{2} \right)^m \left[m \frac{\partial^2 H}{\partial X^2} \left(\frac{\partial H}{\partial X} \right)^{m-1} \right] H^{(m+2)} \quad (159)$$

$$C_2 = (m+2) \left[\frac{2m+2}{2} \right]^m \left(\frac{\partial H}{\partial X} \right)^{m+1} H^{((m+1))} \quad (160)$$

where $R_{\Delta X, \Delta T}(X, T)$ is the residual term which is neglected to solve the numerical problem. Notice that this term can be numerically approximated knowing the solution at the former time step. Now let

$$H_{i,j} = H(X_i, T_j) \quad (161)$$

where X_i and T_j are given by eq.(155), then the finite difference equation to solve, which uses a first order time scheme and a centred second order spatial scheme, is written as

$$H_{i,j+1} = H_{i,j} + \frac{\Delta T}{(\Delta X)^2} \left([H_{i+1,j}]^n + [H_{i-1,j}]^n - 2[H_{i,j}]^n \right) \quad (162)$$

Notice that $H_{0,j+1}$ corresponds to upstream Neumann condition given by eq.(155). It is derived from eq.(161), say $H_{0,j+1} = H_{1,j+1}$.

Also, if i_{\max} denotes the maximum value that subscript i can reach, i.e. i_{\max} is rounded off to the integer that is closest to

$\frac{L + X_e}{\Delta X}$, then downstream Dirichlet condition given by eq.(35) yields

$$H_{i_{\max}, j+1} = 0$$

(200163)

Moreover, adopting the same stability criterion as for the Newtonian fluid, the numerical scheme gave stable results.

5.4 Results

First of all, the similar solution and the numerical solution for the dam-break flow of a power-law fluid obtained previously must be validated in the limiting case of a Newtonian fluid, by comparison with an experimental and theoretical study presented in [12], who obtained a short time viscous regime and a long time viscous regime, respectively described by the following scaling laws

$$X_{fs} \propto T^{1/2}, \quad X_{fl} \propto T^{1/5} \quad (164)$$

These results clearly agree with those of the present work for $n=1$. Moreover, the fluid height at dam site in the short time regime found as $H_d=0.664$ in present

work agrees with the value of $H_d=0.684$ obtained previously in the study of the Newtonian case [12].

Then, the effect of the shear thinning property of the mud will be derived by computing the solution obtained both analytically and numerically. Indeed, the present computations showed that the general characteristics of the flow which were obtained for the Newtonian model are preserved. For any value of the power law index, the shape of the different graphs obtained for Newtonian fluid is preserved, only the slope of the graphs are influenced by n . The general features of the physical description of the development of the dam-break flows of both the water and the mud are similar. Notably, the free surface profile obtained in the Newtonian case is similar to that of the mud, for the short time viscous regime and for the long time regime as well. Meanwhile, the effect of the power-law index on the solution will be pointed out owing to a reference to the Newtonian case.

We computed the different constants appearing in the solution together with different characteristic quantities in the range $0.20 \leq n \leq 1.00$. Recalling that $m = 1/n$, we see that for increasing power law index, the characteristic time decreases. This means that one effect of the shear thinning property is to slow down the back wave. This result means that $|U_b(T)|$ increases with n (see fig. 13). The same remark holds for the velocity of the front wave $U_f(T)$ in both the short time regime and the long time regime. As a consequence, the abscissa of the positive wave $X_f(T)$ increases with the power law index, both for the short time regime and for the long time regime. Meanwhile, for all the tested values of the power law index ($0.2 \leq n \leq 1$), the maximum heights at given station versus the corresponding abscissa were described by a single graph. Concerning the time when H_{\max} occurs at

given station, T_{max} is shorter for larger n (fig. 12).

All these results illustrate the increasing of the velocity of the negative wave and the positive wave with power law index, due to lower friction for the water than for the mud characterized by the same consistency. Furthermore, there was a satisfactory agreement of the results obtained analytically and numerically Focussing on the dam site (figs. 14-19, for $m=1$), abscissa of the dam height at dam site is more close to $x=0$ for the numerical computation than for the analytical calculation. A similar characteristic was observed with all the values tested for m . So, the numerical model seems more accurate than the analytical model, but the results from the two studies remain concordant and satisfactory.

Finally, we found that for decreasing power law index, the critical height H_d decreases, which means that the quantity of fluid mobilized during the short time regime is larger for the mud than for the water. As a consequence, for a structure situated in a vulnerable zone, the impact will occur later for the mud than for the water as stated earlier in this section, but the quantity of fluid will be larger. Moreover, considering that the density of the mud is larger than that of the water, the impact of the mud is expected to be greater and potentially produce more damages. This effect was discussed in [48-50], among others.

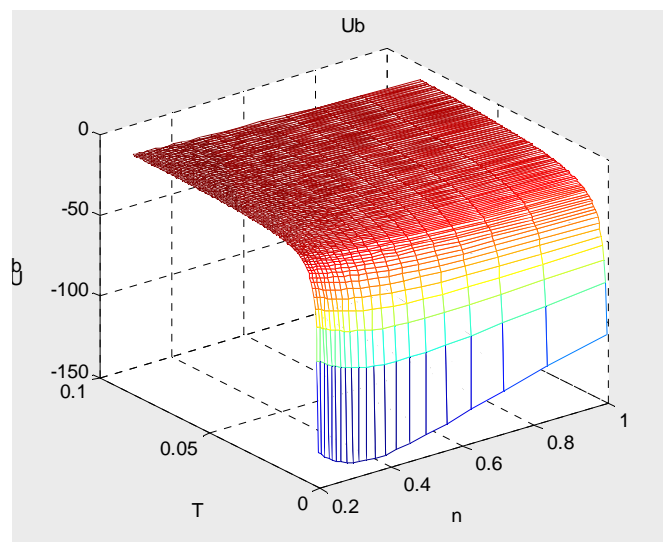


Fig. 12 : Time variation of depression velocity for assigned power law index

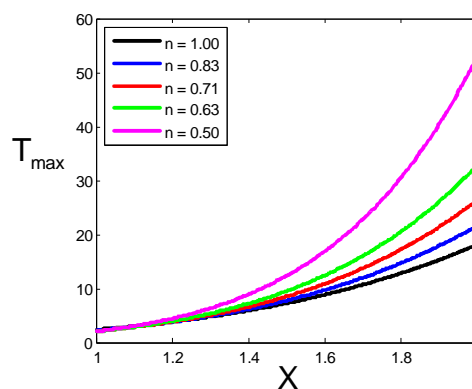


Fig. 13: Variation of the time of occurrence of maximum height for given abscissa for given power law index

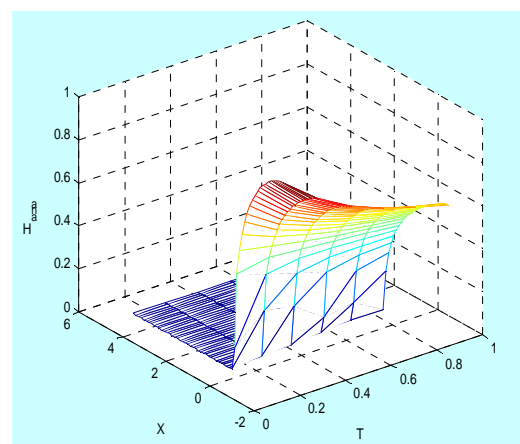


Fig. 14: Fluid height vs. time and abscissa obtained analytically viewed from dam-site

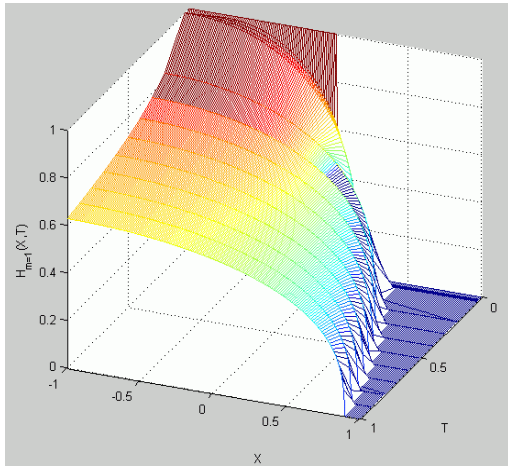


Fig. 15: Fluid height vs. time and abscissa obtained analytically: side-view

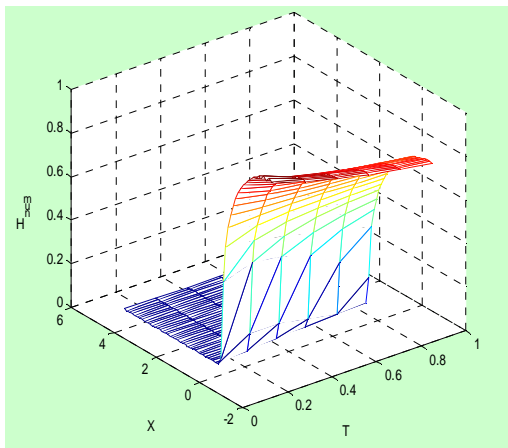


Fig. 16: Fluid height vs. time and abscissa obtained numerically viewed from dam-site

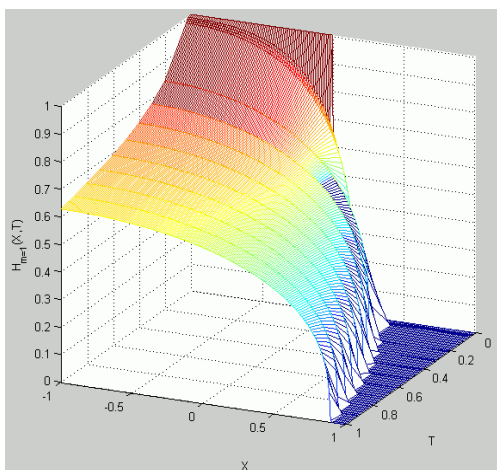


Fig. 17: Fluid height vs. time and abscissa obtained numerically: side-view

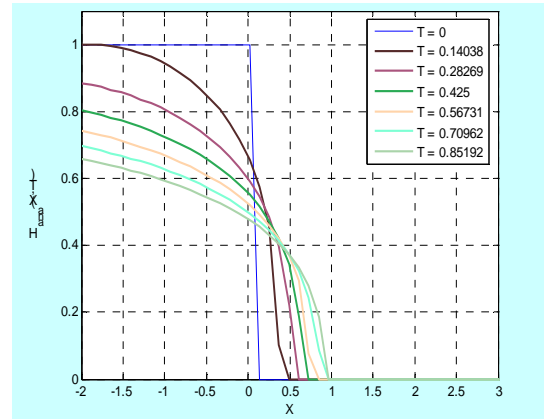


Fig. 18: Zoom on dam site or fluid height vs. time and abscissa obtained analytically

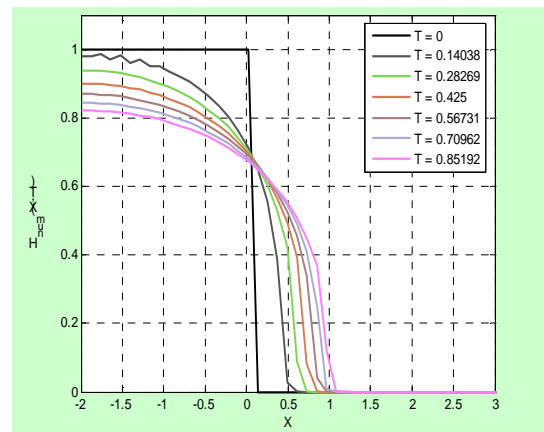


Fig. 19: Zoom on dam site for fluid height vs. time and abscissa obtained numerically

6 CONCLUSION

Flash floods and the debris floods constitute dangerous phenomena for public safety and quality of life. The originality of the present approach is to consider these two flood waves as special cases of a single global model of a dam-break flow of a muddy fluid, depending on the time scale. This unified model was presented in the present paper. For tackling the case where the fluid is muddy, the model was first built in the case of a Newtonian fluid and then generalized using an appropriate rheological behaviour equation.

The flow regimes of the horizontal viscous dam-break flow are well known from experimental studies. At initial time (when the dam collapses), the fluid is released

downstream (positive wave), while a negative wave propagates upstream. The flow is inertial (Ritter's solution) until the back wave reaches the fixed rear wall. Then, the viscous forces become higher than the inertial ones and a short time viscous regime takes place until. In this regime, the flow height at dam site has a (fix) characteristic value. As the reflected wave overtakes the positive wave, the long time or asymptotic regime takes place. The present study considered the modelling of these two viscous flow regimes.

Applying the conservation of mass and momentum with the shallow water approximation, an equation of motion was derived and made non dimensional, when the viscous forces were assumed to be the dominant ones. It was of porous medium type and similar solutions built analytically.

Then, the problem was considered numerically. The previous equation of motion was approximated using an explicit finite difference method. The stability and convergence of the computations were insured using a criteria based on heuristic approach. The very good agreement between the numerical and the analytical solutions showed the consistence of the numerical scheme for both short time and long time solutions. The time evolution of the abscissa and velocities of the different front waves were determined, as well as the different characteristic heights.

A general model of debris flows was developed. Using the assumption of a Herschel-Bulkley behavior scheme, the conservation of mass and momentum equations with the shallow-water approximation were considered without *a priori* values assigned to the rheological parameters. A general equation of motion in a non dimensional form was obtained, which reflects both a Newtonian fluid and a power-law fluid for particular values of the rheological parameters. The general characteristics of this strongly non linear partial differential equation were pointed

out, such as the location of the yield surface and the abscissa of the wave front at the stoppage.

The special configuration of a horizontal dam-break flow was then considered. It is important for environmental engineering and natural risk assessment with regard to mudflow. For the limiting case of an inertial flow, where the inertial effects are dominant, the equation of motion was solved by the method of characteristics. It was pointed out that the flow develops in the form of two waves. A positive wave, propagating downstream with constant speed, associated to a negative one propagating upstream with half that speed. So, it could be pointed out that one effect of the yield stress is to slow down the wave front propagation both in the downstream direction and in the upstream direction with respect to the Newtonian case. Another effect of the yield stress is to state the fluid height at the positive wave front at a value depending on the yield stress, while this height is zero in the Newtonian case.

Finally, considering the equation of motion in the configuration of the equilibrium state where the inertial effects are negligible and the friction stress reduces to the yield stress. the main characteristics of the stoppage were determined, i.e. the depth at the fixed rear wall of the reservoir, the stage at the wave front, and the abscissa of the wave front.

The flow generated by the collapse of a dam retaining a muddy fluid was considered theoretically. The fluid is assumed viscoplastic following a Herschel-Bulkley rheological law. The equations of conservation of mass and momentum were written in a non dimensional form with the shallow water approximation. Assuming the inertial effects dominant against the viscous ones in order to model a flash flood event an equation of motion was built. Then, an implicit equation was formed for the friction slope. The equation of motion could then be solved using the method of characteristics. The law of

propagation of the front of the positive wave was provided, and the back wave as well. The corresponding laws of propagation for the Newtonian fluid and for the power law fluid were recovered when appropriate values of the rheological parameters were used. Piau [33] gave *ad'hoc* similar relations. In this paper, a proof was given of this solution and it is a crucial step for implementing the kinematic wave theory for the muddy fluids [48]-[49] in our model.

The horizontal dam-break flow of mud modeled by a power-law fluid was considered analytically. The channel was smooth and dry at initial time. The solution of such problem depends on the time scale. The inertial regime characterized by dominant inertial forces, takes place immediately after dam collapse, and holds until the negative wave touches the rear wall. In such an inviscid solution (Ritter solution), the rheological behaviour of the mud has no influence. Then, the viscous forces become the dominant forces and a viscous solution is obtained. Applying the conservation of mass and momentum with the shallow water approximation, an equation of motion was derived and made non-dimensional. The analytical and the numerical solution of this viscous flow was worked out in terms of wave front dynamics and spatio-temporal variations in the fluid height, with a self-similar form. The short time solution holds until the wave reflected by the (fixed) rear wall overtakes the front and then the long time one governs the asymptotical flow dynamics and shape. The limiting case of a Newtonian fluid derived from this solution was successfully compared with previous experimental, analytical and numerical solution. Then the shear thinning property of the mud was pointed out. It was notably shown that the general features of the physical description of the development of the dam-break flows of both the water and the mud are similar. Moreover, all these results illustrate the increasing of the velocity of the negative wave and the

positive wave with power law index, due to lower friction for the water than for the mud characterized by the same consistency. Finally, for all the tested values of the power law index ($0.2 \leq n \leq 1$), the maximum heights at given station versus the corresponding abscissa were described by a single graph.

References

- [1] Viollet, P.L., Chabard, J.P., Esposito, P. & Laurence, D.: *Mécanique des Fluides Appliquée*, Presses de l'École Nationale des Ponts et Chaussées, Paris (France), 2002 (in French)
- [2] De Saint-Venant, B., *Théorie du mouvement non permanent des eaux*, C.R. Acad. Sci., 73, 147-154 ; 217-225, 1871 (in French)
- [3] Ritter, A.: *Die Fortpflanzung der wasser wellen*. Ver Deutsch Ingenieure Zeitschrift, Vol.36, N°33, pp. 947-954, 1892 (in German)
- [4] Dressler, R.F., *Hydraulic resistance effects upon the dam-break functions*, J. Res. Nat. Bur. Stand., 49(3), 217-225, 1952
- [5] Dressler, R.F., *Comparison of theories and experiments for hydraulic dam-break wave*, Int. Assoc. Sci. Pubs., 3(28), 319-328, 1954
- [6] Whitham, G.B., *The effects of hydraulic resistance in the dam- break problem*, Proc. Roy. Soc., A(227), 399-407, 1955
- [7] Gill, M.A.: "Dam-break problem." *Encyclopedia of fluid mechanics*, 6, N.P. Cheremisinoff, eds., Gulf, Houston (Texas), 1429-1473, 1987
- [8] Faure, J. & Nahas, N., *Etude numérique et expérimentale d'intumescences à forte courbure du front*, La Houille Blanche, 5, 576-587, 1961 (in French)
- [9] Sakkas, J.G. & Strelkoff, T. : *Dimensionless Solution of Dam-Break Flood Waves*, J. Hydr. Div. (ASCE), 102 (HY2), Proc. Paper 11910, 171-184, 1976
- [10] Katapodes N.D. & Schamber, D.R.: *Applicability of Dam-Break Flood Wave*

- Models, *J. Hydr. Eng. (ASCE)*, 19(5), 702-721, 1983
- [11] Hunt, B.: Newtonian fluid mechanics treatment of debris flows and avalanches. *J. Hydr. Div. (ASCE)*, vol. 120(12), 1350-1363, 1994
- [12] Nsom, B., Ndong, W. & Ravelo, B.: Modelling the Zero-Inertia, Horizontal Viscous Dam-Break Problem, *WSEAS Transactions on Fluid Mechanics*, vol. 3(2), 77-89, 2008
- [13] Nsom, B., Debiante, K. and Piau, J.M.: Bed slope effect in the dam-break problem. *J. Hydr. Res. (IAHR)*, vol. 38(6), 459-464, 2000
- [14] Simpson, J.E. (1987). « Gravity Currents in the Environment and the Laboratory », *John Wiley & Sons*, New York.
- [15] Schwarz, L.W.: Viscous flows down an inclined plane: Instability and finger formation. *Phys. Fluids A*, vol. 1(3), 443-445, 1989
- [16] Barthes-Biesel, D. : Rectification d'un film liquide sous l'effet de la gravité et de la tension superficielle. (in French) <<http://www.enseignement.polytechnique.fr/profs/informatique/Georges.Gonthier/pi98/film.html>> (June 1, 1998)
- [17] Sedov, L.I.: "Similarity and Dimensional Methods in Mechanics", Academic Press, New York, 1959
- [18] Smith, G.D.: "Numerical Solution of Partial Differential Equations", Oxford University Press, New York, 1969
- [19] Forsythe, G.E. and Wasow, W.R.: "Finite-Difference Methods for Partial Differential Equations", John Wiley and Sons, New York, 1967
- [20] Richtmyer, R.D. and Morton, K.W.: "Difference Methods for Initial Value Problems", John Wiley and Sons, New York, 1967
- [21] Weast, R.C., Astle, M.J. and Beyer, W.H., eds. "Handbook of chemistry and physics". CRC, Boca Raton, Fla, 1987.
- [22] Herschel, W.H. and Bulkley, R.: Über die viskosität und Elastizität von Solen. *Am. Soc. Test. Mat.*, 26, 621-633, 1926
- [23] Bagnold, R.A.: Experiments on a gravity-free dispersion of large solid spheres in a Newtonian fluid under shear, *Proc. Roy. Soc. Lond. A*, 225, 49-63, 1954.
- [24] Takahashi, T.: Mechanical characteristics of debris flow, *J. Hydr. Div.*, 104(HY8), 1153-1169, 1978 .
- [25] Savage, S.B. and Hutter, K.: The notion of a finite mass of granular material down a rough incline. *J. Fluid Mech.*, 199, 177-215, 1989
- [26] Bingham, E.C. Fluidity and Plasticity, Mc Graw Hill, New York, 1929.
- [27] Magnin, A. and Piau, J.M. Cone-and-plate rheometry of yield stress fluids. Study of an aqueous gel., *J. Non Newt. Fluid Mech.*, 36, 85-108, 1990
- [28] Nsom, B., Debiante, K., Piau, J.M. and Ayadi, A., Gradually varied flow of unloaded mud in open channel. *Appl. Mech. Engrg.*, 4(3), 443-470, 1999
- [29] Coussot, P. « Steady, laminar flow of concentrated mud suspensions in open channel ». *J. Hydr. Res. (IAHR)*, 32, 535-559, 1994
- [30] Nguyen, Q.D. and Boger, D.V., Yield stress measurement for concentrated suspensions, *J. Rheol.*, 27, 321-349, 1983
- [31] Doraiswamy, D., Mujumdar, A.N., Tsao, I., Beris, A.N., Danforth, S.C. and Metzner, A.B.: The Cox-Merz rule extended: a rheological model for concentrated suspensions and other materials with a yield stress. *J. Rheol.*, 35, 647-685, 1991
- [32] Laigle, D.: Two-dimensional modelling of debris flow spreading on alluvial fans, in "Hydroinformatics'96": 651-657, Balkema, Rotterdam, The Netherlands, 1996
- [33] Piau, J.M.: Flow of a yield stress fluid in a long domain. Application to flow on an inclined plane. *J. Rheol.*, 40: 711-723, 1996
- [34] Cavaillé, Y. and Fortier, M.A. : « Contribution à l'étude de l'écoulement variable accompagnant la vidange brusque d'une retenue » (in French). Publications Scientifiques et Techniques du Ministère

de l'Air, N°410, Paris – France - (in French), 1965

[35] Huppert, H.E.: The propagation of two-dimensional and axisymmetric viscous gravity currents over a rigid horizontal surface. *J. Fluid Mech.*, 121, 43-58, 1982

[36] Gratton, J. and Minotti, F. Theory of creeping gravity currents of a non-Newtonian liquid. *Phys. Rev. E*, 60(6), 6960-6967, 1999

[37] Piau, J.M. and Debiane, K.: Consistometers rheometry of power-law viscous fluids, *J. Non-Newt. Fluid Mech.*, 127, 213-224, 2005

[38] Johnson, P.C. & Jackson, R. (1990). Frictional-collisional equations of motion for particulate flows and their applications to chutes. *J. Fluid Mech.*, 210, 510-535, 1990

[39] Yano, K. and Daido, A.: Fundamental study on mudflows, *Ann. Disaster Prevention Res. Inst. Kyoto Univ.*, 7, 340-347, 1965

[40] Qian, N. and Wan, Z.: A critical Review of the Research on the Hyperconcentrated Flow in China. International Research and Training Centre on Erosion and Sedimentation, Beijing, China, 1986

[41] Ng, C.O. and Mei, C.C.: Roll waves on a shallow layer of mud modelled as a power-law fluid, *J. Fluid Mech.*, 263, 151-183, 1994

[42] Wan, Z.: Bed material movement in hyperconcentrated flow. Series Paper 31. Inst. Hydrodynamics and Hydraulic Engineering, Technical University of Denmark, 1982

[43] Kajiuchi, T. and Saito, A.: Flow enhancement of laminar pulsating flow of Bingham plastic fluids, *J. Chem. Eng. Japan*, 17, 34-38, 1984

[44] O'Brien, J.S. and Julien, P.Y.: Laboratory analysis of mudflow properties., *J. Hydraul. Eng. (ASCE)*, 114(8), 877-887, 1988

[45] Coussot, P. and Proust, S.: Slow, unconfined spreading of mudflow, *J. Geophys. Res.*, 101(B11), 25217-25229, 1996

[46] Wilson, S.D.R. and Burgess S.L.: The steady, spreading flow of a rivulet of mud, *J. Non-Newt. Fluid Mech.*, 79, 77-85, 1998

[47] Huang, X. and Garcia, M.H.: A Herschel-Bulkley model for mud flow down a slope, *J. Fluid Mech.*, 374, 305-333, 1998

[48] Arattano, M. and Savage, W.Z.: Kinematic wave theory for debris flows, U.S. Department of the interior, U.S. Geological Survey, Open-File Report 92-290: 1992-2031, 1992

[49] Arattano, M. and Savage, W.G.: Modeling debris flows as kinematic waves, *Bulletin of the IAEG*, 49: 95-105, 1994

[50] Nsom, B., Piau, J.M., Saramito, P., Debiane & Ayadi, A.: Experimental and numerical study of the viscous dam-break problem, in "Progress and Trends in Rheology-V", Proc. 5th European Conference on Rheology, Portoroz (Slovenia), eds. I. Emri & R. Cvelbar, Springer Verlag (Berlin), p. 157, 1998.